

# THE 4TH INTERNATIONAL CONFERENCE ON ALUMINUM ALLOYS

## PHASE DIAGRAMS AND PHASE EQUILIBRIA

P. Kolby

SINTEF Materials Technology, P.O. Box 124 N-0314, Blindern, Norway.

### Abstract

A comparison between the classical and CALPHAD (Calculation of Phase Diagrams) methods for phase diagram determination and construction has been made. Further the CALPHAD method has been briefly explained. Finally, examples of multi component aluminum phase diagrams of relevance to extrusion and foundry alloys, and to the growing of intermetallic phases, have been calculated using the Thermo-Calc computer code and the COST507 database for light alloy development. Some selected sections through the diagrams are presented with a brief explanation of the interesting aspects of each section.

### Introduction: A Comparison between Classical and Computer Generated Phase Diagrams

Classically, sections of phase diagrams have been constructed by conducting a number of experiments and the drawing of lines through these experimentally determined points. Since the number of experimental points needed is limited, this method has proven very effective when applied to binary systems, such as the Al-Mg system displayed in Fig. 1. It can therefore be said that when experiments are free from error, the classical method for phase diagram construction works well for binary systems. Indeed the equilibrium liquidus, solidus and solvus can be read directly from Fig. 1. By constructing a tieline and applying the lever rule, the composition and fractions of the different phases present in a binary Al-Mg alloy can also be determined.

The same procedure can in principle be applied to a ternary system, such as the Al-Mg-Si system, but the number of experiments necessary to get insight into the phase diagram is dramatically increased. Yet such work has been done successfully, on a limited number of sections, as is shown in a number of phase diagram books (for example Phillips [1]). A problem arises, however, when one begins to use these ternary diagrams. Even though binary alloy phase diagrams are relatively easy to use, provided only temperature and composition vary, the step up to a ternary system begins to be difficult to master. The main problem is the isopleth or vertical sections. The all important tielines (or conodes) are very rarely located in the plane in such a section. This means that a point on the liquidus surface in one section will not usually be in equilibrium with a point on the solidus in the same section. This results in the lever rule not being applicable to a ternary isopleth in the same way as in a binary system. The effect is illustrated by inspecting Fig. 2a and b. Fig. 2a shows an isopleth section at constant 1 wt% Si through the Al-Mg-Si system. If this was a binary phase diagram one could simply draw a line perpendicular to the temperature axis between the liquidus and the solidus surfaces to find the relative proportions and compositions of the solid and the liquid at the temperature of interest. However since this is a

ternary diagram, care must be taken. The constant temperature line at 600°C in Fig. 2a would suggest that a solid with the composition A is in equilibrium with a liquid of composition B. This is a gross error, as the isothermal section at 600°C presented in Fig. 2b clearly illustrates. In fact the liquid with composition B is in equilibrium with a solid with composition C.

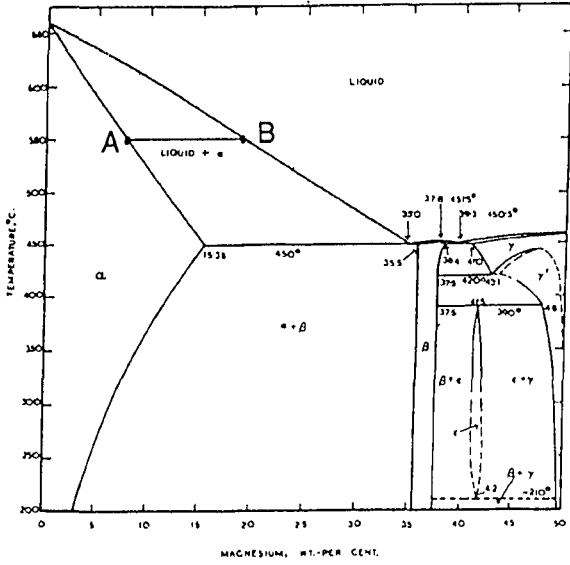


Figure 1. The Al-Mg phase diagram from Phillips [1].

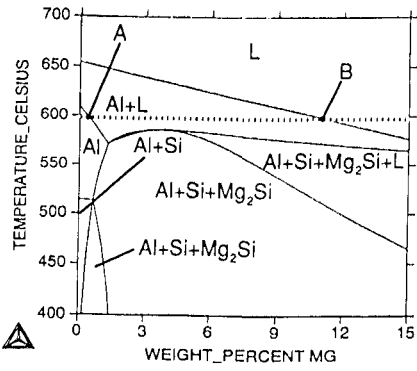


Figure 2a). An isopleth section through the Al-Mg-Si system at constant 1% Si.

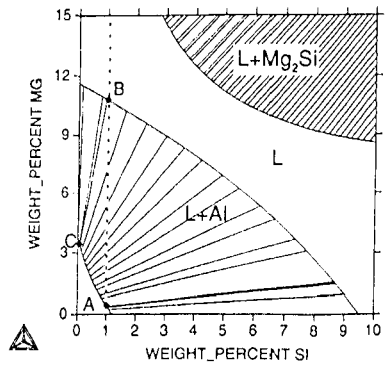


Figure 2b). The isothermal section at 600°C through the Al-Mg-Si phase diagram with tie-lines drawn in. Note that the tie lines are not in the plane of Fig. 2a.

The situation becomes even more complex in a quaternary system. Here the tie-lines are not in the plane in any two dimensional section through the 4 dimensional phase diagram. Great success has, however, been achieved in displaying the liquidus surface in a 4 dimensional system. The method used by Dons in Langsrud [2], gives a clear image of the liquidus surface, and the technique is equally applicable to the solidus and solvus surfaces. Such a diagram is shown in Fig. 3. However, it is not trivial to visualise how the matrix composition varies between two isothermal sections in the diagram and very difficult to follow a specific alloy composition from the liquid state to room temperature.

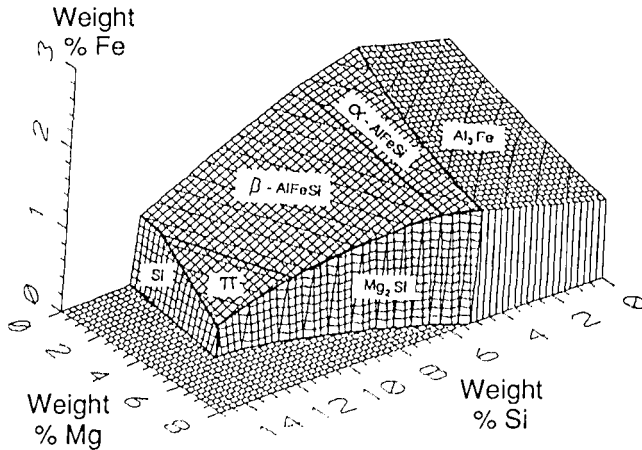


Figure 3. The region of the liquidus surface of the quaternary Al-Mg-Fe-Si phase diagram where Al is the primary precipitate. (Courtesy of A. L. Dons)

In a quinary (five component) or higher order system, it is virtually impossible to get the information desired about a specific alloy without having access to very special sections through the phase diagram. The CALPHAD method, which is discussed in the next section, and the database storage of thermodynamic parameters, allows a user to specify a temperature and composition of the alloy in question, and get a complete picture of the equilibrium situation, meaning everything from the composition and amount of different phases present to the total enthalpy of the system. This represents a dramatic increase in the availability of phase diagram information, not only to experts in the field of phase diagrams, but to scientists at all levels.

Another problem with the classical method for phase diagram determination is the ability to acquire a sufficient amount of experimental data. If steps of 0.1 wt % in the composition of each alloying element, and temperature steps of 25°C were used in a set up to experimentally determine the five component Al-Mg-Mn-Fe-Si phase diagram, it would be necessary to make about 200 million samples to map the region from 0-2%Fe, 0-2%Mn, 0-20%Si and 0-10%Mg between the temperatures of 0 and 800°C. Many of these castings would of course not be critical to get a reasonably good overall picture of the system, but several parameters would need to be determined for each casting, making the total amount of work mindboggling. This is not taking into account the extremely slow kinetics encountered in systems containing Mn and/or Fe, which will necessitate rapid solidification, cold deformation, and tremendously long annealing times to reach equilibrium (see Kolby and Sigli [3]).

Obviously the task of experimentally determining the Al-Mg-Mn-Fe-Si phase diagram is not practically achievable, without some scheme to minimise the amount of data needed to describe the system. This is achieved by the use of thermodynamic principles. It is well known that phase diagrams can be generated by using the principle of minimisation of the total Gibbs energy of a system (see for example Verhoven [4]). Therefore, if some method of modelling the Gibbs energy of each phase involved in a system is utilised, the phase diagram can be generated by minimising the total Gibbs energy of the system. This is a tremendously powerful tool in reducing the 200 million plus experiments otherwise required to map the system. The CALPHAD method (see the section on the CALPHAD method in this article) is a method used to model the Gibbs energy of a phase, and it therefore provides the aluminium industry with a means of getting 200 million castings worth of information from a permille or even permicro of the experiments. Even though interest most often is limited to a very small region around the specifications of a particular alloy it is the overview of the complete system that enables a user to choose the optimal composition and thermal treatments to achieve a set of desired properties. This means that the aluminium company of the future will have to have a precise knowledge of multicomponent phase diagrams to be competitive, both economically and environmentally. This aspect is magnified further by the introduction of a large amount of recycled metal, containing a large number of elements, to the market. In other words the setting of standards for recycled multicomponent alloys will require an in-depth knowledge of phase diagrams with up to 10 components.

### The CALPHAD method

The search for more precise and rational means of evaluating, representing and storing phase diagram information has culminated in the development of computer codes such as Thermo-Calc [5, 6], F\*A\*C\*T [7, 8], MTDATA [9, 10], and many others which all build on the so-called CALPHAD method. The CALPHAD method for phase diagram assessment is a two step process. First a choice of a suitable model for the chemical composition of each phase involved in the system must be made. This model incorporates any possible deviation from stoichiometry.

The Gibbs energy of this phase will then be defined by the energy of the endpoints (in composition) of the phase. As an example take  $\alpha$ -AlMnSi. This phase is modelled as stoichiometric in manganese, which is a good assumption in the Al-Mn-Si system where no Fe is present, but can vary in silicon between the limits of Al<sub>18</sub>Mn<sub>4</sub>Si<sub>1</sub> to Al<sub>16</sub>Mn<sub>4</sub>Si<sub>3</sub>. The Al rich and Si rich endpoints of this phase will have a Gibbs energy described by equation 1 and 2 respectively, where a, b, c, d and k, m, n, p are parameters to be fitted using experimental data, and T is the temperature in Kelvin.

$$G(\text{Al}_{18}\text{Mn}_4\text{Si}) = a + b*T + c*T*\ln(T) + d*T^2 + \dots \quad (1)$$

$$G(\text{Al}_{16}\text{Mn}_4\text{Si}_3) = k + m*T + n*T*\ln(T) + p*T^2 + \dots \quad (2)$$

The Gibbs energy of the  $\alpha$  phase with an intermediate composition, such as for example Al<sub>17</sub>Mn<sub>4</sub>Si<sub>2</sub>, is constructed as the weighted sum of the two energies listed in equations 1 and 2. To this result the energy associated with the entropy of ideal mixing ( $S_m$ ) and an interaction term (L) to describe deviations from ideal mixing is added. Both the entropy and interaction terms are dependent on the composition in such a way that they are equal to zero at the end points of the phase [11]. The resultant equation for the Gibbs energy of the Al<sub>17</sub>Mn<sub>4</sub>Si<sub>2</sub> compound is shown in equation 3 and a graphic representation is shown in Fig. 4.

$$G(\text{Al}_{17}\text{Mn}_4\text{Si}_2) = 0.5*G(\text{Al}_{18}\text{Mn}_4\text{Si}) + 0.5*G(\text{Al}_{16}\text{Mn}_4\text{Si}_3) + S_m + L \quad (3)$$

A number of different models exist, such that several different effects can be reproduced. Examples are models incorporating ordering and magnetic effects to mention the most commonly used.

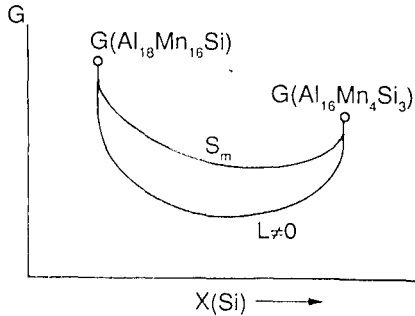


Figure 4. A graphical sketch of the effect of the different terms on the Gibbs energy curve.

It is well known that equilibrium, and thereby phase diagrams, can be constructed by drawing common tangents to the Gibbs energy curves involved in the system. This scheme functions well in binary and ternary systems where the common tangent is generally a line and a plane, respectively. Drawing the common tangent is however difficult in a higher order system, since in this case both the tangent and the Gibbs energy curve is generally multi dimensional. We therefore need to introduce the chemical potential ( $\mu$ ) to deal with higher order systems. The chemical potential with respect to element  $i$  is defined in equation 4, where  $G$  is the Gibbs energy and  $n_i$  is the concentration of element  $i$  in the alloy. Equation 4 reveals that the chemical potential is the derivative of the Gibbs energy with respect to the content of one alloying element, under the condition that the temperature, the pressure and the concentration of all the other alloying elements are kept constant.

$$\mu_i = \frac{\partial G}{\partial n_i} \quad (4)$$

It can be shown (see for example Prince [12]) that at equilibrium the chemical potential of each element must be equal in all the phases involved in the equilibrium situation. In simpler words this means that all the individual directional derivatives of each Gibbs energy curve of relevance to the equilibrium in question must be equal. This principle is nothing more than a mathematical method for "drawing" the common tangent, and is applicable to the construction of multi component phase diagrams.

The CALPHAD method of modelling the Gibbs energy of a phase allows extrapolations and interpolations into hitherto unknown regions of a phase diagram, and into new alloy systems. The result is the ability to calculate the phase diagram of higher order commercial systems. It should be noted that commercial aluminium alloys are at least ternary systems, since Si and Fe are always present as impurities in commercial aluminium. Most of the tonnage is in fact some Al-Mg-Si or Al-Mg-Mn alloys, which, when including the Fe and Si impurities, comprise the Al-Mg-Mn-Fe-Si system. There are also a wide range of alloys which contain more than five components.

To be able to combine the Gibbs energy descriptions of phases evaluated as parts of different alloy systems, for example Al from the unary Al system, Si from the unary Si system and  $Mg_2Si$

from the binary Mg-Si system to allow calculations on the Al-Mg-Si ternary system, it is critical that the Gibbs energy descriptions of these phases all have the same reference level. Another element that must be chosen with care if compatibility is desired, is the model for non-stoichiometric phase. Take for instance the Al<sub>6</sub>Mn and Al<sub>6</sub>Fe phases. It is critical to be sure that the Al<sub>6</sub>Mn and Al<sub>6</sub>Fe phases have the same model in the binary Al-Mn and Al-Fe systems to allow them to be combined into the Al<sub>6</sub>(Mn,Fe) when going to the ternary Al-Mn-Fe system. Since Gibbs energy is not an absolute quantity, an organisation called SGTE (Scientific Group Thermodata Europe) make recommendations on which reference level and models to use to ensure compatibility.

When the Gibbs energy surface has been mathematically described allowing for variations in composition, this description can be used to extrapolate into higher order systems. Take for example the stoichiometric Mg<sub>2</sub>Si compound. It is generally accepted that the solubility of Al, Mn and Fe in this phase is negligible. It is therefore considered a good approximation to say that the Mg<sub>2</sub>Si compound found in Al alloys has one and only one fixed composition. Since Mg<sub>2</sub>Si does not dissolve any of the mentioned elements the mathematical expression for the Gibbs energy of the Mg<sub>2</sub>Si compound is independent of the content of these elements in the system, as shown in Equation 5 (The appearance of equation 5 is taken from [13]).

$$G(\text{Mg}_2\text{Si}) = a + b \cdot T + c \cdot T \cdot \ln(T) \quad (5)$$

This means in practise that the Gibbs energy surface of Mg<sub>2</sub>Si in the Al-Mg-Si-Mn-Fe system is completely described by equation 5. The parameters in equation 5 are all determined during the assessment of the Mg-Si binary system. By the same reasoning crystalline Si is completely described by the assessment of the unary Si system, since its ability to take other elements of interest in aluminum alloys into solid solution is negligible. The  $\alpha$ -AlMnSi phase, also commonly referred to as  $\alpha$ -Al(Mn,Fe)Si because Fe can replace most of the Mn in this phase, is, however, not completely described before the quaternary Al-Mn-Fe-Si system is assessed. In other words the amount of work needed to add one component to an evaluated system will decrease as the amount of components increases. Therefore, reliable extrapolations into multicomponent aluminum systems can be calculated after the ternary and, in a few cases, the quaternary subsystems are evaluated.

At this point it is necessary to stress that the calculated phase diagrams are only as good as the experimental data used to evaluate them. However, if a number of experimental data points are available, the assessment process can tell you whether one series of experimental results can be thermodynamically compatible with the results of a different investigation in another but related part of the diagram. An example of this is presented by Kolby and Sigli in these proceedings [3]. In short, the values used by Phillips [1] for the solubility of Mn in solid Al at 550°C is impossible to reconcile with the position of the apex of the Al+Al<sub>6</sub>Mn+ $\alpha$ -AlMnSi 3-phase field in the Al-Mn-Si system in the same reference. It is impossible to adjust the Gibbs energy surfaces of the Al and Al<sub>6</sub>Mn phases such that the phase boundary between the Al and Al+Al<sub>6</sub>Mn phase fields in the Al-Mn-Si diagram of Phillips is reproduced. This is explained by thermodynamics as follows; When thermodynamic principles are employed one is reminded that the phase boundary between the Al and Al+Al<sub>6</sub>Mn phase fields must be very close to parallel to the silicon axis. This is because Al<sub>6</sub>Mn does not dissolve appreciable amounts of Si, meaning that, to explain a dramatic deviation from a horizontal boundary between the Al and Al+Al<sub>6</sub>Mn phase fields would require a non physically high effect of Si on the activity of Mn in solid Al. Other, more subtle errors in experimental investigations can also be revealed.

### The COST507 action

Gathering and critically reviewing the available experimental information, combined with the optimisation of the parameters describing the Gibbs energy surfaces of the phases of interest, constitutes a substantial amount of work, which no single aluminum company, research institute or University could hope to achieve, on a reasonable time scale, for a multicomponent system. A substantial portion of the aluminum companies in Europe, have therefore joined forces with several Universities and research institutions in the COST507 action on constructing a thermodynamic database for light alloy development. The COST507 action is now in its second round and has set out to construct a database that allows calculations in several key aluminum systems by the end of 1996. These systems are listed in Table I.

Table I. The Key Aluminum Systems for Assessment by COST507 Round II 1994-1997.

Key System	System Manager
Al-Mg-Mn-Fe-Si	P. Kolby, SINTEF Materials Technology, Oslo, Norway
Al-Mg-Si-Cu	Dr. M. Jacobs, RWTH Aachen, Germany
Al-Mg-Cu-Zn	Prof. H. L. Lucas, Max Planck Institute, Stuttgart, Germany
Al-Li-Cu-Mg-Zr	Prof. M. Hämmäläinen, Helsinki University of Technology, Espoo, Finland
Ti-Al-Metal	Dr. B. Sundman, Royal institute of Technology, Stockholm, Sweden
Ti-Al-Non-metal	Dr. T. G. Chart, National Physical Laboratory, London, United Kingdom

Even though the amount of experimental information necessary to map a system is dramatically reduced when thermodynamic modelling is introduced, there is a problem of a lack of experimental data in aluminium systems making it difficult to describe the Gibbs energy curves sufficiently well. In some cases the available data are very inaccurate or even misinterpreted, an effect which, as already discussed, may be uncovered by the assessment process, but needs rechecking experimentally.

The COST507 community is now in the process of conducting an experimental program parallel to the modelling of the Al-Mg-Mn-Fe-Si system, in some cases to supplement existing data to increase the accuracy of the thermodynamic evaluation of a system, and in other cases, to acquire the data needed to evaluate a system at all. Similar work is also being done on the other key systems shown in Table I. For some critical or difficult experiments a policy of duplication of the measurements by two independent laboratories, using different techniques is being applied. The solvus measurements are, for example, being conducted in a close collaboration between Pechiney CRV and SINTEF Materials Technology. Some results of this collaboration are presented in these proceedings [3].

All the binary and most of the important ternary subsystems of the Al-Mg-Mn-Fe-Si system have been completed within the COST 507 program. This enables preliminary extrapolations to quaternary systems to be made. Comparing the extrapolations to data points found in the literature enables us to construct an efficient experimental study for checking the accuracy of the calculated phase diagram. These findings can then be employed to improve the calculated diagrams. After a few such iterations the result is a means to access any part of the phase diagram to get out any thermodynamically determined parameter. This convenient way to get any phase diagram information can form the basis for a more general program modelling kinetic aspects, which would enable calculations of the evolution of the microstructure during solidification and especially homogenisation.

#### Example: Application of the Calculations to Extrusion Alloys

The 6xxx series alloys are commonly used as extrusion billets. It has long been believed that the  $\beta$ -AlFeSi is not desired in the billet during extrusion, probably because of its detrimental mechanical properties. Unfortunately this phase is nearly unavoidable during casting. It is widely believed that the transformation of  $\beta$ -phase to  $\alpha$ -AlFeSi that takes place during homogenisation treatment is needed in order to improve extrudability, but obviously also other desired microstructural changes take place during homogenisation. Let us take a look at the conditions which have to be fulfilled to achieve the  $\beta$  to  $\alpha$  phase transition.

Naturally the temperature for this heat treatment should be as high as possible so as to facilitate a more rapid diffusion of Fe. It is, however, also important to avoid local melting. To avoid the  $\beta$  phase a low silicon content is recommended, but to increase the T6-strength, the Si (and Mg) content should be above a lower limit. The phase diagram presented in Fig. 5 shows the 580°C isothermal of the ternary Al-Fe-Si system. Fig. 5 shows that the silicon content is the critical factor in determining whether the  $\beta$  or  $\alpha$  phases is the equilibrium precipitate, but a slight dependence on Fe is also seen. The alloy does however also contain Mg and in many cases Mn. Therefore extrapolations based on the existing ternary subsystems of Al-Mg-Mn-Fe-Si have been made. These systems are Al-Mg-Si [13], Al-Mn-Si [14], and Al-Fe-Si [15]. Fig. 6 shows the effect of adding 0.9 wt% Mg (which is the upper limit in the AA6063 alloy) on the Al-Fe-Si phase diagram presented in Fig. 5. Fig. 6 clearly justifies the common assumption that it is sufficient to look at the Al-Fe-Si system when concerned with the  $\beta$  to  $\alpha$  transition during homogenisation. The effect of adding 0.1 wt% Mn, which is the maximum limit in AA6063, to the Al-Fe-Si-0.9Mg system should also be given some attention. This Mn addition would perhaps stabilise the cubic  $\alpha$ -Al(Mn,Fe)Si compound to an extent where it appears in the phase diagram as an equilibrium precipitate. In fact it has been observed by Dons [16] that a mixture of the cubic and hexagonal alpha phases exists after homogenisation of Al-Mg-Fe-Si-Mn alloys containing less than 0.1 wt% Mn. This could be explained if the alloy lies in a 3 phase field where both modifications of  $\alpha$  are precipitated at the composition in question at 580°C. The phase boundaries presented in Fig. 6 would therefore probably be displaced such that the boundary marking the limit for the existence for  $\beta$ -AlFeSi is moved towards higher Si contents. It is, however, impossible to get a convincing answer to the question of how a small content of Mn will affect the Al-Fe-Mg-Si phase diagram without introducing Fe solubility in the  $\alpha$ -AlMnSi phase, and perhaps also Mn solubility in the  $\beta$ -AlFeSi phase. This is one of the upcoming tasks for the COST507 action.

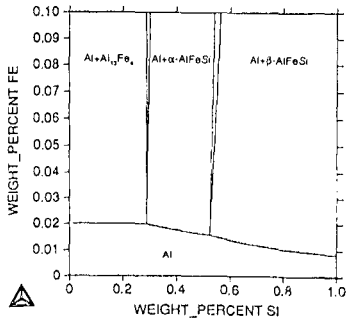


Figure 5. The isothermal section at 580°C of the ternary Al-Fe-Si system.

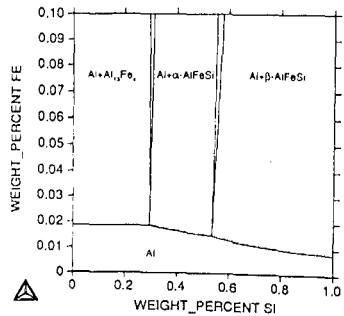


Figure 6. The isothermal section at 580°C, and 0.9 wt% Mg of the quaternary Al-Mg-Fe-Si system.

The maximum limits of Mg and Si in AA6063 are 0.9 wt% and 0.6 wt%, respectively. Fig 5 shows us that for this composition at 580°C a Fe content exceeding 0.35 wt% is necessary to be located in the 2 phase  $\alpha$  + Al field. Fig 7 shows the isothermal section at 600°C for the mentioned composition. It can be seen that at this temperature the alloy lies within the  $\alpha$ +Al field at more moderate Fe contents, but there is an increased risk of local melting during heating to this temperature, because of  $Mg_2Si$  and Si formed at the end of solidification during casting.

It can be seen that the upper limit of the AA6063 standard (0.6 wt% Si and 0.9 wt% Mg) is, according to the calculations made here, not a desirable composition if the  $\beta$  phase is to be avoided. At this composition the alloy is in the two phase Al+  $\beta$ -AlFeSi at Fe contents below 0.1 wt% and 580°C. Some degree of transformation of  $\beta$ - to  $\alpha$ -AlFeSi will take place at Fe contents between 0.1 and 0.4 wt%, while the Fe content has to exceed 0.4 wt% for the alloy to be completely inside the Al+ $\alpha$ -AlFeSi phase field at 580°C.

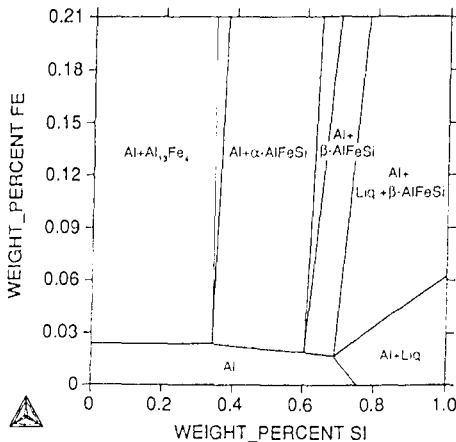


Figure 7. The isothermal section at 600°C and 0.9 wt% Mg of the quinary Al-Mg-Mn-Fe-Si system.

The lower limit, however, has a quite large region above 550°C where  $Al_{13}Fe_4$  is the equilibrium phase. To get  $\alpha-AlFeSi$  one would need to homogenise below this temperature in order not to also precipitate  $Al_{13}Fe_4$ . This balance could, however, be displaced by the introduction of Mn to the alloy. At this point it is important to stress that the standards of the AA6063 alloy are undoubtedly built on a vast amount of experience, which of course should be given precedence over these calculations. The point is, however, that the years of experimental efforts needed to acquire this insight could have been dramatically reduced if the calculation tool discussed here had been available.

Thermodynamic calculations can also be used to investigate other effects encountered in AA6063 extrusion billets. In this respect it is of interest to look at the equilibrium phase distribution as a function of temperature for both the high and the low alloyed version of AA6063. Fig. 8 shows the equilibrium phase distribution as a function of temperature in the high alloyed case. Based on Fig. 8 it can be concluded that at high temperature it is the  $\alpha-AlFeSi$  phase which is stable while as the temperature is decreased the  $\beta$  phase takes over as the stable precipitate. Finally at typical ageing temperatures it is the  $Mg_2Si$  and  $\beta$  phases which are the equilibrium precipitates.

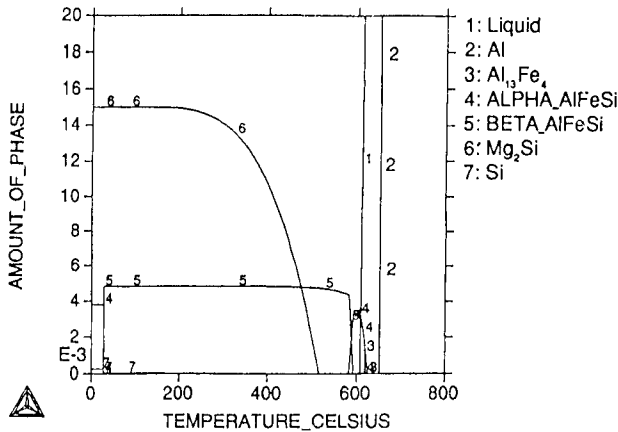


Figure 8. The amount of each phase present as a function of temperature, assuming equilibrium conditions, for an alloy containing 0.9 wt% Mg, 0.6 wt% Si, and 0.15 wt% Fe.

The equilibrium phase distribution for the lower limit of the AA6063 alloy (shown in Fig. 9) also requires some commentary. At high temperatures the  $Al_{13}Fe_4$  (also called  $Al_3Fe$ ) phase is the equilibrium precipitate. As the matrix becomes saturated with Si it becomes necessary to transform the  $Al_{13}Fe_4$  phase, which dissolves little Si, to  $\alpha-AlFeSi$ . Upon decreasing the temperature further the matrix seeks to lower the Si content even further, but all available Fe is bound by the  $\alpha$  phase. A transformation from  $\alpha$  to  $\beta$  (the  $\beta$  phase dissolves more silicon per Fe atom than  $\alpha$ ) takes place. A further decrease in temperature leads to a saturation of the matrix with respect to Mg. This is dealt with by transforming the  $\beta$  phase back to  $\alpha$ , thereby liberating Si for the formation of  $Mg_2Si$ . The final transformation reaction is from  $\alpha$  to  $Al_{13}Fe_4$  in order to liberate more Si as the need to precipitate Mg containing phases increases. It should of course be emphasised that the precipitation sequence shown in Fig. 9 would never run to completion during industrial processing. In this case the situation at 580°C would remain unaltered with respect to the Fe containing precipitates, while some precipitation of  $Mg_2Si$  would occur.

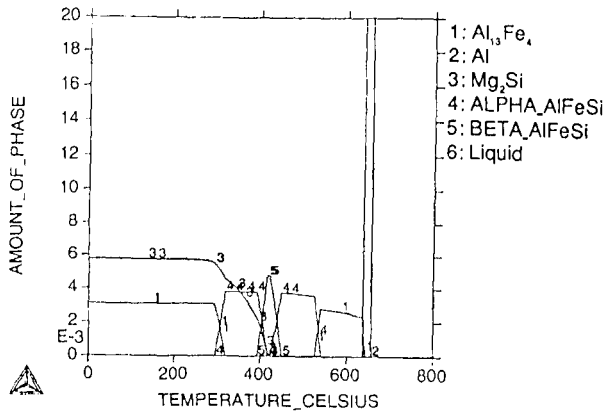


Figure 9. The amount of each phase present as a function of temperature, assuming equilibrium conditions, for an alloy containing 0.45 wt% Mg, 0.2 wt% Si, and 0.15 wt% Fe.

The final example discussed in this section on AA6063 is the difference in precipitation hardening potential between the lower and the upper limit for the AA6063 alloy. The Fe content is assumed to be 0.15 wt%. The equilibrium phase distribution for the Al-0.9Mg-0.6Si-0.15Fe and Al-0.45Mg-0.2Si-0.15Fe alloys is shown in Fig. 8 and 9 respectively. Naturally it is observed that the precipitation of Mg<sub>2</sub>Si begins at a higher temperature in the high alloyed case. Another aspect is the hardening potential itself. For the high alloyed case the amount of Mg<sub>2</sub>Si precipitated at equilibrium conditions at 180°C, is more than twice that observed in the low alloyed version of AA6063. As mentioned, no change in the fractions and compositions of the Fe containing precipitates is expected, meaning in effect that the hardening potential shown in Fig. 9 is too high. This is because Si is the limiting component in the low alloyed case. It has been demonstrated in the discussion of Fig. 9 that a series of transformations of Fe containing phases take place in order to regulate the silicon concentration in the matrix. If these transformations are inhibited by kinetic aspects the amount of Si available for precipitation of Mg<sub>2</sub>Si is lowered. This effect will not influence the high alloyed case dramatically since the Si content in the Fe containing phases stable at 580°C is not very different from that observed at the ageing temperature.

Another aspect to note here is that the hardening phase is in fact not the equilibrium Mg<sub>2</sub>Si phase, but a metastable modification commonly called β''. Even though the solvus with respect to the metastable β'' will be moved towards higher contents of the elements in the matrix compared to the equilibrium solvus between Al and Mg<sub>2</sub>Si, this reduction of hardening potential would affect the low alloyed case, which is closer to the solvus, relatively more than the high alloyed case, where the distance to the solvus is greater. This aspect could also be dealt with if a Gibbs energy model for the β'' was available.

#### Example: Application of the Calculations to foundry alloys.

High silicon AlSiMg alloys are used to cast individual aluminum components. The strength of these components can improve through precipitation hardening. The component is generally solution heat treated between 500 and 550°C and subsequently aged at 150-170°C to achieve the

desired precipitation of the  $\beta''$  modification of  $Mg_2Si$ . The success of the ageing process is, however, strongly dependent on the amount of Mg in solid solution after the solution heat treatment. Calculations have therefore been made to investigate the mechanism limiting the solubility of magnesium in solid aluminum at 500 and 550°C.

As previously mentioned all commercial purity aluminum alloys are plagued by Fe impurities of the order of 0.1 wt% Fe. It is therefore necessary to make calculations in the quaternary AlMgSiFe system to shed light on the issue in question. Fig 10 and 11 show the isothermal sections at 500 and 550°C through the Al10SiMgFe system respectively. Please note the excellent comparison between the experimentally determined (see Langsrud [17]) and calculated position of the point labelled A in the diagrams. Fig 10 and 11 clearly show that the solubility of Mg is limited in both cases by the  $\pi$ -AlMgFeSi phase and not by the  $Mg_2Si$  compound as perhaps is expected. Another interesting observation is that the phase boundary between the phase fields containing Al+Si+ $\beta$ -AlFeSi and Al+Si+ $\beta$ -AlFeSi+ $\pi$ -AlMgFeSi is practically vertical, which means that the equilibrium content of Mg in solid solution is independent of the amount of Fe present in the alloy.

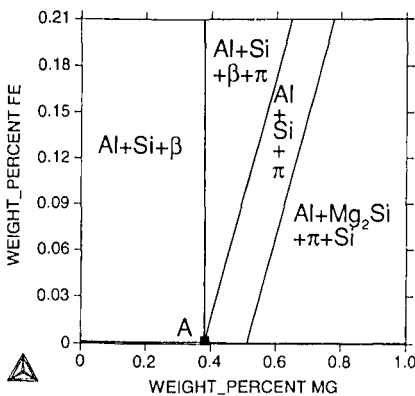


Figure 10. The isothermal section at 500°C, and 10 wt% Si of the quaternary Al-Mg-Fe-Si system. The experimentally determined location (from Langsrud and Brusethaug [17]) of the point labelled A is drawn in for comparison.

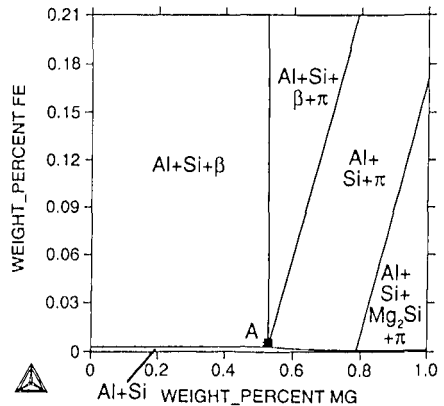


Figure 11. The isothermal section at 550°C, and 10 wt% Si of the quaternary Al-Mg-Fe-Si system. The experimentally determined location (from Langsrud and Brusethaug [17]) of the point labelled A is drawn in for comparison.

Fig 12 shows the equilibrium phase distribution as a function of temperature for the Al10.3Si0.55Fe0.53Mg alloy, which is a typical composition based on secondary aluminum. As is expected based on the discussion of Fig 10 and 11, it is clearly seen that in the temperature range between the solidus and 400°C it is the  $\pi$ -AlMgFeSi phase which consumes the Mg which is not in solid solution. At the ageing temperature the equilibrium situation is, however, one where  $Mg_2Si$  takes the place of  $\pi$ -AlMgFeSi as the most stable Mg containing phase. The consequence of this is that the  $\pi$  phase must be removed. Since  $\pi$  contains Fe, which is a slow diffusing element, it is not possible to dissolve this phase, it needs to be transformed to  $\beta$ -AlFeSi. This process liberates both Mg and Si which in turn react to form  $Mg_2Si$  and Si crystals.

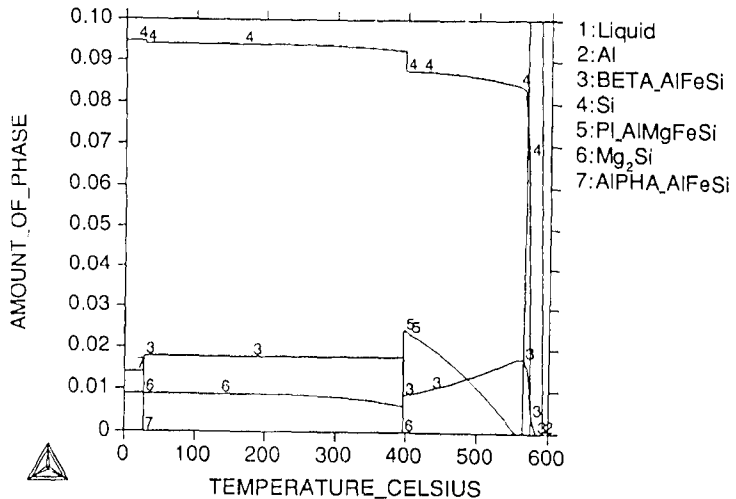


Figure 12. The amount of each phase present as a function of temperature, assuming equilibrium conditions, for an alloy containing 0.53 wt% Mg, 10.3 wt% Si, and 0.55 wt% Fe.

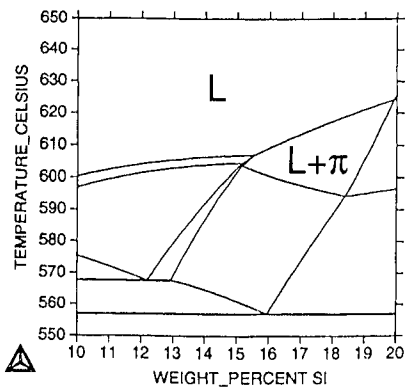
The practical consequence of this observation regards the ideal solution heat treatment temperature. It seems most reasonable to solution heat treat at a temperature where the amount of  $\pi$  phase is at an absolute minimum. This would minimise the need to transform  $\pi$  to  $\beta$ -AlFeSi during the final heat treatment, an effect which would most certainly prolong the ageing time needed in order to reach the precipitation hardening potential. A problem in fulfilling this goal is, however, the proximity of the temperature at which the  $\pi$  phase dissolves completely to the solidus temperature, meaning that local melting may occur when solution heat treating at the "ideal" temperature. A compromise must therefore be made between minimising the amount of  $\pi$  phase present after solution heat treatment and minimising the risk of local melting.

#### Example: Application to Finding the Conditions for Growing Intermetallic Phases

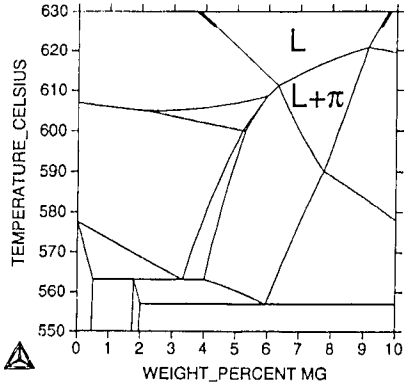
The need to determine the mechanical, electrical and corrosive properties of the phases precipitated in commercial aluminum alloys is beginning to emerge. It is therefore of interest to know how to grow large crystals of the desired phase in a most convenient way. The ideal composition and temperature for particle growth must be determined. The ideal composition will be one where the phase in question is primary over the largest possible temperature interval, so that the precipitation of other phases does not interfere with the growth of the phase of interest as the temperature is slowly decreased. In this respect the phase diagram functions as a map of which window in composition and temperature, is the ideal one.

Another interesting application of thermodynamic calculations thereby becomes apparent, namely finding the ideal composition for the production of millimetre size crystals of the  $\pi$  phase. By calculating a number of isopleth (the amount of one of the elements and the temperature may vary) sections through the Al-Fe-Mg-Si quaternary phase diagram, an impression of where the  $\pi$  phase is primary is achieved. The next step is to investigate how variations in the amount of the different

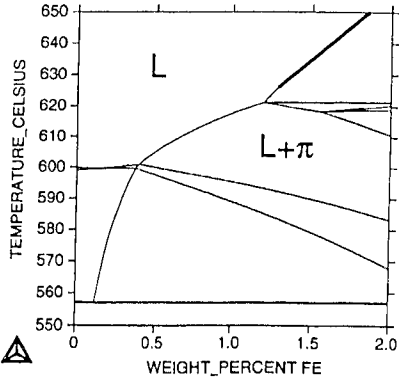
elements affect the size of the region of interest. The composition of the alloy is optimised by choosing the content of each element which maximises the size of the region where  $\pi$  is the primary precipitate. The final iteration in this process is shown in Fig. 13. This process resulted in the choice of alloy composition being Al18Si1Fe8Mg. Fig. 14. shows that, for the mentioned alloy composition, the  $\pi$  phase can be grown in the approximate temperature range between 615°C and 595°C without interference from any other precipitates and also gives some indication of the possible yield. Note, however, that the temperature range is checked by Differential Thermal Analysis (DTA) before the growth procedure is initiated. These thermodynamic calculations have been used to determine the composition of an alloy used to successfully grow the  $\pi$  phase from the liquid [19], and have thereby contributed to substantially minimising the expense of this experimental investigation.



a) at constant 1 wt% Fe and 8 wt% Mg.



b) at constant 1 wt% Fe and 18 wt% Si.



c) at constant 8 wt% Mg and 18 wt% Si.

Figure 13. Isoleth sections through the Al-Mg-Fe-Si system.

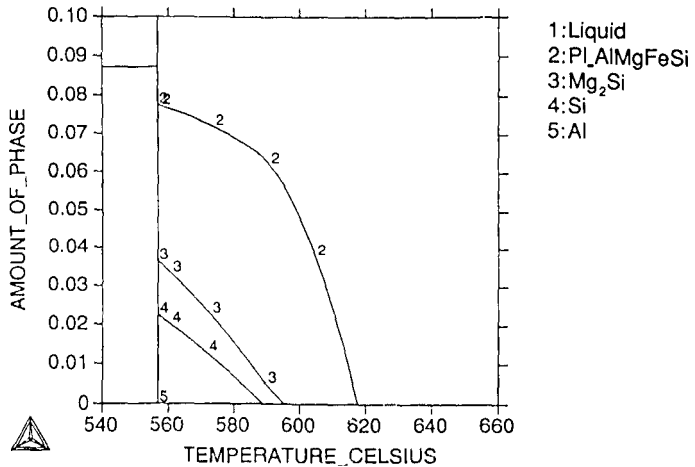


Figure 14. The equilibrium phase distribution, as a function of temperature, for an alloy containing 18 wt% Si, 1 wt% Fe, and 8 wt% Mg.

### Conclusion

The COST 507 efforts in modelling phase diagrams has clearly resulted in a dramatic increase in the availability of consistent phase diagram data for important commercial aluminum systems. It has also been shown that extrapolations can be made on a much more sound basis than previously when only printed data on phase diagrams were available. The full potential of these thermodynamic calculations, are however, only beginning to be realised. The extrapolations that are possible today, form a crucial element in the modelling of metallurgical effects that are based on interpretations of phase diagrams. An example is the modelling of precipitation and phase transformations during homogenisation. When kinetic aspects can be described, calculations of solidification, homogenisation and segregation will also be possible.

With the introduction of more and more recycled metal, it will become increasingly important to set standards, both for composition and heat treatment of alloys exceeding 5 components. In this work the extrapolations made using thermodynamic calculations will certainly be an invaluable tool.

### Acknowledgements

The author acknowledges that the Norwegian contribution to COST507, and thereby this work is financed by Hydro Aluminium A/S, Elkem Aluminium ANS, SINTEF Materials Technology and the Research Council of Norway. The author would also like to thank his partners in the COST507 action for a fruitful collaboration and Y. Langsrud of SINTEF Materials Technology for his support and many valuable suggestions pertaining to the examples presented in this paper.

## References

1. H. W. L. Phillips, Annotated Equilibrium Diagrams of Some Aluminium Alloy Systems (The institute of Metals, 1959).
2. Y. Langsrud et al., The 3rd International Conference on ALUMINIUM ALLOYS, Their Physical and Mechanical Properties, 1, (Editors: Arnberg, Lohne, Nes and Ryum, Trondheim, 1992), 15.
3. P. Kolby and C. Sigli, "Solubility Limit of Mn and Si in Al-Mn-Si at 550°C.", These Proceedings.
4. J. D. Verhoven, Fundamentals of physical metallurgy (John Wiley & sons, 1975).
5. B. Sundman, B. Jansson, and J.-O. Andersson, CALPHAD 2 (1985), 153.
6. B. Sundman, Int. symp. on Computer Software in Chemical and Extractive Metallurgy. Proc. Metall. Soc. of CIM, 11 (Montreal 1988) 75.
7. W. T. Thompson et al., Int. symp. on Computer Software in Chemical and Extractive Metallurgy. Proc. Metall. Soc. of CIM, 11 (Montreal 1988) 87.
8. W. T. Thompson, A. D. Pelton and C. W. Bale, F\*A\*C\*T Facility for the Analysis of Chemical Thermodynamics. Guide to Operations. (McGill University Computing Centre, Montreal 1985).
9. T. I. Barry et al. MTDATA Handbook: Documentation for the NPL Metallurgical and Thermochemical Databank. (National Physical Laboratory, Teddington U.K. 1987)
10. A. T. Dinsdale et al. Int. symp. on Computer Software in Chemical and Extractive Metallurgy. Proc. Metall. Soc. of CIM, 11 (Montreal 1988) 59.
11. M. Hillert, Computer Modelling of Phase Diagrams. (Editor: L. H. Bennett, The Metallurgical Society, Inc. 1986)
12. A. Prince, Alloy Phase Equilibria, (Amsterdam: Elsevier Publishing Company, 1966)
13. N. Chakraborti and H. L. Lukas, CALPHAD 16, (1992), 79.
14. P. Kolby, Unpublished work (1993)
15. M. E. Seiersten, Unpublished work (1993)
16. A. L. Dons, Private Communications 26th August 1994.
17. Y. Langsrud and S. Brusethaug, International GIFA Congress Metal Casting 94, (Dusseldorf 1994) 333.
18. L. F. Mondolfo, Aluminum Alloys: Structure and Properties, (Butterworths, London 1976)
19. C. J. Simensen, To be Published.